Cortical volume and 40-Hz auditory-steady-state responses in patients with schizophrenia and healthy controls

Sungkean Kim[a,b], Seon-Kyeong Jang[a], Do-Won Kim[c], Miseon Shim[d], Yong-Wook Kim[a,b], Chang-Hwan Im[b], Seung-Hwan Lee[a,e,*]

[a] Clinical Emotion and Cognition Research Laboratory, Inje University, Goyang, Republic of Korea
[b] Department of Biomedical Engineering, Hanyang University, Seoul, Republic of Korea
[c] Department of Biomedical Engineering, Chonnam National University, Yeosu, Republic of Korea
[d] Department of Psychiatry, University of Missouri-Kansas City, Kansas City, MO, USA
[e] Department of Psychiatry, Inje University, Ilsan-Paik Hospital, Goyang, Republic of Korea

ARTICLE INFO

ABSTRACT

Background: Abnormalities in the 40-Hz auditory steady-state response (ASSR) of the gamma range have been reported in schizophrenia (SZ) and are regarded as important pathophysiological features. Many of the previous studies reported diminished gamma oscillations in SZ, although some studies reported increased spontaneous gamma oscillations. Furthermore, brain morphological correlates of the gamma band ASSR deficits have rarely examined. We investigated different measures of the 40-Hz ASSR and their association with brain volumes and psychological measures of SZ.

Methods: The 40-Hz ASSR was measured for 80 dB click sounds (1 ms, 500-ms trains at 40-Hz, with 3050 to 3500 inter-train interval) using electroencephalography with 64 electrodes in 33 patients with SZ (male: 16, female: 17 (age range: 21–60)) and 30 healthy controls (HCs) (male: 13, female: 17 (age range: 23–64)). Four gamma oscillation measures (evoked power, spontaneous oscillations (baseline and total power), and inter-trial phase coherence (ITC)) were assessed. The source activities of the ASSR were also analyzed. Brain volumes were assessed using high-resolution magnetic resonance imaging and voxel-based morphometry and superior temporal gyrus (STG) volume measures were obtained.

Results: Patients with SZ had larger total and evoked powers and higher ITC than HCs. Both groups showed significantly different association between mean evoked power and right STG volume. In HCs but not SZ, mean evoked power showed significant positive correlation with right STG volume. In addition, the two groups showed significantly different association between verbal fluency and mean evoked power. High evoked power was significantly correlated with poor verbal fluency in SZ.

Conclusions: The current study found increased gamma oscillation in SZ and suggests significant involvement of the STG in gamma oscillations.

1. Introduction

The 40-Hz auditory steady-state response (ASSR) measures the ability of a neural population to entrain to repeating auditory stimulation at gamma-band frequency (Picton et al., 2003). Gamma-band oscillations help establish temporal precision in local cortical networks (Uhlhaas and Singer, 2010), and are candidate mechanisms of perceptual integration, attentional selection, and working memory (Salinas and Sejnowski, 2001; Tallon-Baudry and Bertrand, 1999). Abnormal gamma oscillations are critical elements of current disease models of

schizophrenia (SZ), including the *N*-methyl-D-aspartate receptor (NMDAR) hypofunction and GABAergic dysfunction models (Sivarao et al., 2016). Gamma oscillation generation is thought to depend on the integrity of neural circuits involving fast-spiking parvalbumin (PV)-expressing cells and NMDAR activation on interneurons, whose alteration is suspected to underlie psychosis (Kantrowitz and Javitt, 2010; Lewis et al., 2012). Specifically, the network of GABAergic interneurons and the negative feedback interaction between pyramidal cells and fast-spiking PV interneurons are hypothesized to be a key circuitry responsible for gamma band oscillations (Uhlhaas and Singer, 2010). As

can be seen, gamma oscillation mechanisms have been relatively well-articulated in animal model studies (Buzsáki and Wang, 2012), and the 40-Hz ASSR has been represented as promising targets in translational research (McNally and McCarley, 2016).

Previous studies on the 40-Hz ASSR have reported reductions in the evoked power and phase-locking measures (i.e., inter-trial phase coherence (ITC)) in patients with SZ (Thuné et al., 2016), though the results are not entirely consistent. For instance, Hong et al. (Hong et al., 2004) demonstrated enhanced evoked power in patients with SZ taking atypical antipsychotics. Hamm et al. (Hamm et al., 2012) also reported higher phase-locking measures in patients with SZ compared to HCs. The authors employed novel stimulus parameters, including broadband auditory noise and a wide inter-stimulus interval (ISI). A recent new line of research investigating spontaneous (non-phase locked) gamma-band activity levels found enhanced gamma activity, both during the ASSR stimulus presentation and the task baseline (Hirano et al., 2015). These findings may correspond with animal studies reporting an association between NMDAR hypofunction and increased spontaneous gamma power (Ehrlichman et al., 2009; Korotkova et al., 2010), and together indicate the need to investigate the mechanisms and clinical implications of different ASSR measures.

Only a few studies have explicitly distinguished the ASSR measures. Mathalon and Sohal (Mathalon and Sohal, 2015) classified the ASSR measures into stimulus-evoked oscillations (evoked power), stimulus-induced oscillations (total power), and stimulus-independent oscillations (baseline or resting-state power). Evoked power reflects bottom-up sensory encoding, while spontaneous gamma power (stimulus-induced and stimulus-independent oscillations) is related to emerging dynamic processes in cortical networks (Jadi et al., 2016). In addition to distinct ASSR measures, experimental parameters and sample characteristics may have contributed to the previous discrepant results. For example, studies differed in their ISI and sex ratio (Hamm et al., 2012; Hong et al., 2004), and other factors including handedness and attentional manipulation could have influenced the results (Griskova-Bulanova et al., 2018; Melynte et al., 2018).

While the relationship between brain anatomical alterations and the 40-Hz ASSR deficits may provide a potential explanation for the pathophysiology of SZ, there are limited studies on this topic. Previous studies have localized the generator of the 40-Hz ASSR in the primary auditory cortex in the superior temporal gyrus (STG) and in subcortical and cerebellar regions (Gutschalk et al., 1999; Herdman et al., 2002). There is evidence for anatomical alterations of pyramidal cells in the primary auditory cortex of SZ (Dorph-Petersen et al., 2009; Sweet et al., 2003), and the 40-Hz ASSR could be associated with gray matter loss and symptom severity in SZ (Gupta et al., 2015). To date, only one study has examined the relationship between the 40-Hz ASSR and the thickness of the STG in SZ (Edgar et al., 2014). This study found a positive correlation between the 40-Hz ASSR and left STG thickness in a healthy population but not in patients with SZ. More studies need to investigate the association between 40-Hz ASSR deficits and brain anatomy in SZ, especially with potentially different measures of the 40-Hz ASSR and a sample consisted of different demographic composition (e.g., ratios of included men and women and diverse cultural backgrounds).

In this study, we aimed to examine how different measures of the 40-Hz ASSR (Mathalon and Sohal, 2015) are altered in SZ. We also sought to investigate the link between the 40-Hz ASSR functions and brain structural abnormalities in SZ. This was done by examining the correlation between the sensor and source level 40-Hz ASSR activities and gray matter volume alterations in the STG. Finally, to further understand the clinical and functional significance of the 40-Hz ASSR, we examined whether the 40-Hz ASSR is associated with cognitive and social functioning in SZ.

2. Material and methods

2.1. Participants

A total of 33 patients with SZ (male: 16, female: 17, age: 42.21 ± 10.99 (range: 21–60)) were recruited and assessed for Axis I (First et al., 1996) and II (First et al., 1997) disorders, based on the Structured Clinical Interview for the Diagnostic and Statistical Manual of Mental Disorders, 4th edition (SCID). Their psychiatric symptoms were evaluated using the Positive and Negative Syndrome Scale (PANSS) (Kay et al., 1987). No patient had a lifetime history of central nervous system disease, alcohol or drug abuse, mental retardation, or head injury with loss of consciousness, and no patient had current Axis II disorders. All patients were receiving atypical antipsychotic medication at the time of testing.

A total of 30 healthy controls (HCs) (male: 13, female: 17, age: 43.33 ± 12.95 (range: 23–64)) were recruited from the local community through newspapers and flyers. An initial screening interview excluded subjects with any identifiable neurological disorder, head injury, or any personal or family history of psychiatric illness. After the initial screening, potential HCs were interviewed using the SCID for Axis II Psychiatric Disorders (First et al., 1997) and were excluded if they had any of these disorders. All subjects signed a written informed consent form approved by the Institutional Review Board of Inje University Ilsan Paik Hospital, Republic of Korea (2015-07-23).

2.2. Psychological measures

Psychological measures and scales were used to measure neurocognition and functional outcome. To evaluate neurocognition, the Trail Making Test-A & −B (TMT-A & TMT−B) (Seo et al., 2006), verbal fluency test (Lezak, 2004), and Korean-Auditory Verbal Learning Test (K-AVLT) (Kim, 1999) were applied. In the TMT-A, participants were asked to draw lines sequentially connecting 25 consecutive, encircled numbers distributed across a sheet of paper within 360 s. In the TMT-B, participants were instructed to draw lines alternating between numbers and Korean letters within 300 s (Seo et al., 2006). The TMT-A and TMT-B, which were scored according to the time taken to complete the task, mainly evaluated visual attention and executive functioning, respectively. Longer time scores indicated worse performance. In the verbal fluency test, the participants named as many animals as possible within 60 s. This task evaluates verbal production and semantic memory abilities (Lezak, 2004). The Korean-Auditory Verbal Learning Test (K-AVLT), which is included in the Rey-Kim Memory Test (Kim, 1999), is a verbal memory test that consists of five immediate recall trials (trials 1–5), plus delayed recall and delayed recognition trials. The immediate recall score is the sum of words (trials 1–5) recalled correctly. The delayed recall score indicates the number of words recalled correctly after a delay period of 20 min. The delayed recognition score indicates the correctly chosen words in the original list (15 words) spoken by the examiner among a list of 50 words after delayed recall.

To assess functional outcome, the Social Functioning Questionnaire (SFQ) (Kim et al., 2015; Zanello et al., 2005) and Social and Occupational Functioning Assessment Scale (SOFAS) (Goldman et al., 1992; Lee et al., 2006) were applied. The SFQ (Zanello et al., 2005) is a 16-item self-report instrument, which assesses both frequency (eight items) and satisfaction (eight items) with various social behaviors enacted during the 2 weeks preceding the assessment. This measure yields the following separate indices of social functioning: frequency, satisfaction, and global. Higher scores indicate worse social functioning. The SOFAS was used as a one-item rating scale for Axis V (i.e. the clinician's judgment of overall level of functioning) in the Diagnostic and Statistical Manual for Mental Disorders, 4th Edition. The SOFAS is a global rating of current functioning, ranging from 0 to 100, with lower scores representing lower functioning (Goldman et al., 1992; Lee et al., 2006).

2.3. Auditory stimuli and procedures

Participants were seated in a comfortable chair in a quiet, shielded room in front of a computer screen (Mitsubishi, 22-in. CRT monitor). They were instructed to look at the fixation cross on the monitor with their eyes open while listening to auditory stimuli. The auditory stimuli were presented binaurally through MDR-D777 headphones (Sony, Tokyo, Japan). The auditory stimuli were click sounds (80 dB, 1 ms) that were presented in 500-ms trains at 40-Hz. Click sound trains were presented in a single block containing 150 trains. The inter-train interval was randomized between 3050 and 3500 ms. The experiment required approximately 10 min to complete. The stimuli were generated by *E*-Prime software (Psychology Software Tools, Pittsburgh, PA, USA).

2.4. Electroencephalography recording and preprocessing

The electroencephalography (EEG) recording was synchronized to stimulus presentation onset by E-Prime. EEG was recorded using a NeuroScan SynAmps amplifier (Compumedics USA, Charlotte, NC, USA), with 64 Ag-AgCl electrodes mounted on a Quik-Cap, using an extended 10–20 placement scheme. The ground electrode was placed on the forehead and the physically linked reference electrode was attached to both mastoids. The vertical electrooculogram (EOG) channels were positioned above and below the left eye, while the horizontal EOG channels were recorded at the outer canthus of each eye. The impedance was maintained below 5 kΩ. All data were recorded with a 0.1–100 Hz band pass filter and a 60 Hz notch filter, with a sampling rate of 1000 Hz.

The recorded EEG data were preprocessed using CURRY 7 (Compumedics USA, Charlotte, NC, USA). The EEG data were re-referenced to an average reference. Gross artifacts, such as movement artifacts, were rejected by visual inspection by a trained person who had no prior information regarding the data origin. Artifacts related to eye movement or eye blinks were removed using the mathematical procedure implemented in the preprocessing function (Semlitsch et al., 1986) of the CURRY 7 software. Data were then epoched from the 300 ms pre-stimulus to the 1000 ms post-stimulus. The baseline correction was performed using the pre-stimulus period. The epochs were rejected if they contained significant physiological artifacts (amplitude exceeding ± 75 μV) in any site over 62 electrodes. The number of epochs of ASSR used for the analysis did not significantly differ between patients with SZ and HCs (SZ: 116.03 ± 23.73; HC: 120.07 ± 27.20, $p = .532$).

2.4.1. Time-frequency analysis

To measure spectral power, an event-related spectral perturbation (ERSP) analysis was applied to the recorded EEG signals. ERSP was calculated using functions implemented in a well-known MATLAB toolbox EEGLAB (http://sccn.ucsd.edu/eeglab/) (Delorme and Makeig, 2004; Moore et al., 2012).

Spectral power was calculated using the short-time Fourier transform every 5 ms, with a Hanning window size of 250 ms for each trial. No smoothing or filtering process was applied to generate the resultant ERSP maps. The power spectrum of each trial was then normalized with respect to the average power of the baseline period (−300 to 0 ms) to probe for changes in the spectral power values before and after stimulus onset. The normalized power spectra were then averaged over trials, which resulted in baseline-normalized ERSP maps and total power for each individual. Evoked power was also calculated as the spectral power of the averaged single epochs using the short-time Fourier transform as above. Evoked power measures the power of the average evoked potential in which the contribution of non-stimulus locked activity is minimized. Furthermore, spectral power was computed during the baseline period (baseline power). The short-time Fourier transform was applied to the single trial epochs, and the single trial power spectra were averaged for the baseline power spectrum. Power values,

including total, evoked, and baseline power, were $10 \times \log_{10}$ transformed (Kiebel et al., 2005).

In addition to spectral power, the inter-trial phase coherence (ITC) was calculated, which measures the similarity in the phase of oscillatory activity across individual trials, independent of the signal amplitude. The ITC was quantified by dividing the complex output of the ERSP by its complex norm (absolute value), which was then averaged across trials. The complex norm of this averaged value resulted in the ITC value for different time and frequency points. ITC values ranged from 0 (i.e., non-phase locked, random activity across trials) to 1 (i.e., activity that is fully locked in phase across individual trials at a given latency). We used the ERSP and ITC as measures of power and phase, respectively, since these parameters provided information about the temporal dynamics of ASSR.

The mean baseline power was calculated at the Cz electrode by averaging the data over the baseline period (−300 to 0 ms) for 36–45 Hz. The mean total and evoked power and mean ITC were calculated at the Cz electrode by averaging the data over the first 500 ms within a trial (0–500 ms) for 36–45 Hz (Krishnan et al., 2009; Tallon-Baudry et al., 1996). For the time-course analyses, we calculated the mean total and evoked power and mean ITC for each 100-ms epoch (i.e., 0–100, 100–200, 200–300, 300–400, and 400–500 ms) (Light et al., 2006; O'donnell et al., 2004).

2.4.2. Source imaging

Standardized low-resolution brain electromagnetic tomography (sLORETA) was used to compute the cortical distribution of the standardized source current density of the 40-Hz ASSR. sLORETA is a representative source-imaging method for solving the EEG inverse problem (Pascual-Marqui, 2002), which assumes that the source activation of a voxel is similar to that of the surrounding voxels for calculating a particular solution and applies an appropriate standardization of current density. The lead field matrix was computed using a realistic head model segmented based on the Montreal Neurological Institute (MNI) 152 standard template, wherein the three-dimensional solution space was restricted only to the cortical gray matter and hippocampus (Fuchs et al., 2002). The solution space is composed of 6239 voxels with a 5-mm resolution. Anatomical labels, such as the Brodmann areas, were provided by using an appropriate transformation from MNI to Talairach space (Brett et al., 2002).

The source image of the ASSR was analyzed in the baseline period (−300–0 ms) and auditory-stimulus period (0–500 ms) for 36–45 Hz. Three types of source image for the ASSR were estimated. First, the source images of each trial in the auditory-stimulus period were calculated and averaged (i.e., total source activity). Second, the source image of each averaged single epoch was calculated (i.e., evoked source activity). Third, the source images of each trial in the baseline period were calculated and averaged (i.e., baseline source activity). The region of interest (ROI) of the ASSR source activities in this study was the STG, a region well known to be associated with the 40-Hz ASSR and interneuron deficits (Edgar et al., 2014). The source measure for phase locking was not calculated, since it is not reasonable to use phase information of power obtained from sLORETA.

2.5. Magnetic resonance imaging acquisition and voxel-based morphometry

Magnetic resonance imaging (MRI) was performed using a 1.5 T scanner (Magneton Avanto, Siemens, Erlangen, Germany). Head motion was minimized by using restraining foam pads provided by the manufacturer. A high-resolution T1-weighted MRI volume dataset was acquired with the following; acquisition parameters of a 227×384 acquisition matrix, a 210×250 field-of-view, $0.9 \times 0.7 \times 1.2$ voxel size, a total of 87,168 voxels, an echo time (TE) of 3.42 ms, a repetition time (TR) of 1900 ms, 1.2 mm slice thickness, and a flip angle of 15˚.

The voxel-based volumetry (VBM) was conducted using Computational Anatomy Toolbox (CAT12; developed by Christian

Gaser, University of Jena, http://dbm.neuro.uni-jena.de/cat) with the SPM12 software package (Wellcome Department of Cognitive Neurology, London, UK) (Ashburner, 2009; Ashburner and Friston, 2000). The structural T1 images were registered to an ICBM East Asian template and normalized using the DARTEL algorithm (Ashburner, 2007). The images were then segmented into gray matter, white matter, and cerebrospinal fluid (Ashburner and Friston, 2005). Jacobian transformed tissue probability maps were used to modulate images to obtain volume differences in gray matter. The volume of the regions was extracted using the Neuromorphometrics atlas, available in SPM 12, provided by Neuromorphometrics, Inc. (http://neuromorphometrics.com). The STG was analyzed as an ROI of brain volume.

2.6. Statistical analysis

For statistical analyses, independent t-tests were used to compare the demographic data, psychological measures, and mean baseline power at Cz between the patients with SZ and the HCs. A repeated-measures analysis of variance (ANOVA) was performed separately with 5 time-blocks (0–100, 100–200, 200–300, 300–400, and 400–500 ms) as the within-subjects factors, and the groups (i.e., SZ and HC) as the between-subjects factors for total and evoked power and ITC at Cz. Furthermore, a repeated-measures ANOVA was performed separately with hemisphere (left and right) as the within-subjects factors and the groups as the between-subjects factors for the source activities of the ASSR and the volume of the ROI. When volume was included in the analysis, the total intracranial volume (TIV) was considered as a covariate to correct for different brain sizes (Segall et al., 2008). When a significant effect was found, post-hoc comparisons were performed using an independent t-test or Bonferroni correction or a univariate ANOVA with TIV as a covariate.

The relationship between the 40-Hz ASSR sensor and source measures and STG volume was analyzed using hierarchical regression analyses with a 5000 bootstrap resampling technique to correct for multiple correlations. The bootstrap test is a weaker method than the Bonferroni test for solving the multiple comparison problem; however, the robustness and stability of the bootstrap test have been recognized by various previous studies (Haukoos and Lewis, 2005; Pernet et al., 2013; Ruscio, 2008). Further, the bootstrap test has been widely used in EEG analysis (Kim et al., 2016; Pernet et al., 2011). Analogous analyses were computed for the 40-Hz ASSR sensor and source measures and the psychological measures. Differences with a $p < .05$ (two-tailed) were deemed to be statistically significant. Statistical analyses were performed using SPSS 21 (SPSS, Inc., Chicago, IL, USA).

3. Results

3.1. Demographic and psychological characteristics

Table 1 shows the demographic and psychological characteristics of the SZ and HC groups. The verbal fluency and K-AVLT-delayed recall scores were significantly higher in the HC compared with the SZ group (verbal fluency: 15.91 ± 4.84 vs. 19.00 ± 5.82, $p = .027$; K-AVLT-delayed recall: 6.31 ± 3.65 vs. 9.89 ± 2.08, $p < .001$, respectively). No other significant differences were found.

3.2. 40-Hz sensory activity at Cz

There was no significant difference between the groups with regard to the mean baseline power (−3.33 ± 2.79 vs. −3.24 ± 2.42, $p = .896$). For total power, a significant group-by-time interaction revealed a greater total power in the later than in the earlier time blocks. Also, there were significant group differences (SZ > HC) only in the time blocks after 200 ms ($ps < 0.01$). For evoked power, a significant main effect of group showed a group difference (SZ > HC) in the mean

Table 1
Demographic characteristics of patients with SZ and HCs.

	SZ (N = 33)	HC (N = 30)	p
Age (years)	42.21 ± 10.99	43.33 ± 12.95	0.711
Sex			
Male	16 (48.5)	13 (43.3)	0.682
Female	17 (51.5)	17 (56.7)	
Premorbid IQ	103.03 ± 9.86	107.85 ± 9.34	0.059
Education (years)	13.85 ± 2.06	13.87 ± 3.81	0.982
Number of hospitalization	2.82 ± 3.30		
Duration of illness (years)	13.57 ± 8.90		
Onset age (years)	27.83 ± 9.83		
Dosage of antipsychotics (chlorpromazine equivalent, mg)	495.06 ± 558.53		
Positive and negative syndrome scale			
Positive	13.06 ± 6.57		
Negative	16.45 ± 6.19		
General	29.61 ± 8.30		
Total	59.12 ± 18.93		
TMT-A (seconds)	31.28 ± 13.35	28.38 ± 10.24	0.351
TMT-B (seconds)	107.47 ± 53.55	84.97 ± 50.40	0.108
Verbal fluency	15.91 ± 4.84	19.00 ± 5.82	0.027
K-AVLT – delayed recall	6.31 ± 3.65	9.89 ± 2.08	< 0.001
SFQ	44.88 ± 11.96	40.14 ± 7.77	0.066
SOFAS	63.73 ± 13.59		

HC, healthy control; IQ, intelligence quotient; K-AVLT, Korean Auditory Verbal Learning Test; SFQ, Social Functioning Questionnaire; SOFAS, Social and Occupational Functioning Assessment Scale; SZ, schizophrenia; TMT-A, Trail Making Test-A; TMT-B, Trail Making Test-B.

evoked power (0–500 ms) ($p < .05$). In addition, a significant main effect of time showed greater evoked power in the later than in the earlier time blocks ($p < .001$). However, there was no significant group-by-time interaction ($p > .05$). For ITC, a significant main effect of group showed a group difference (SZ > HC) in the mean ITC (0–500 ms) ($p < .05$). In addition, a significant main effect of time showed greater ITC in the later than in the earlier time blocks ($p < .001$). However, there was no significant group-by-time interaction ($p > .05$). Fig. 1 shows the grand average time-frequency maps and time course for total power, evoked power, and ITC at Cz in the 40-Hz frequency for the SZ and HC groups.

3.3. 40-Hz source activity

None of source activities in the STG showed a significant main effect of group or group-by-hemisphere interaction. For the baseline source activity of the STG, the main effect of hemisphere (left > right) was significant ($p < .05$). The main effect of group and the interaction term were not significant ($p > .05$). For the total and evoked source activities of the STG, the main effects of hemisphere (left > right) were significant ($ps < 0.05$). The main effects of group and the interaction terms were not significant ($ps > 0.05$).

3.4. MRI volume

In this study, there was no significant difference between the groups regarding TIV. For STG, there was a marginally significant main effect of group ($F (1, 58) = 3.782$, $p = .057$). However, there were neither a significant main effect of hemisphere ($F (1, 58) = 2.584$, $p = .113$) nor group-by-hemisphere interaction ($F (1, 58) = 1.158$, $p = .286$). A post-hoc analysis revealed that the volume of the STG (left and right averaged) was marginally smaller in patients with SZ compared to HCs (6.19 ± 0.95 vs. 6.55 ± 0.88, $p = .057$).
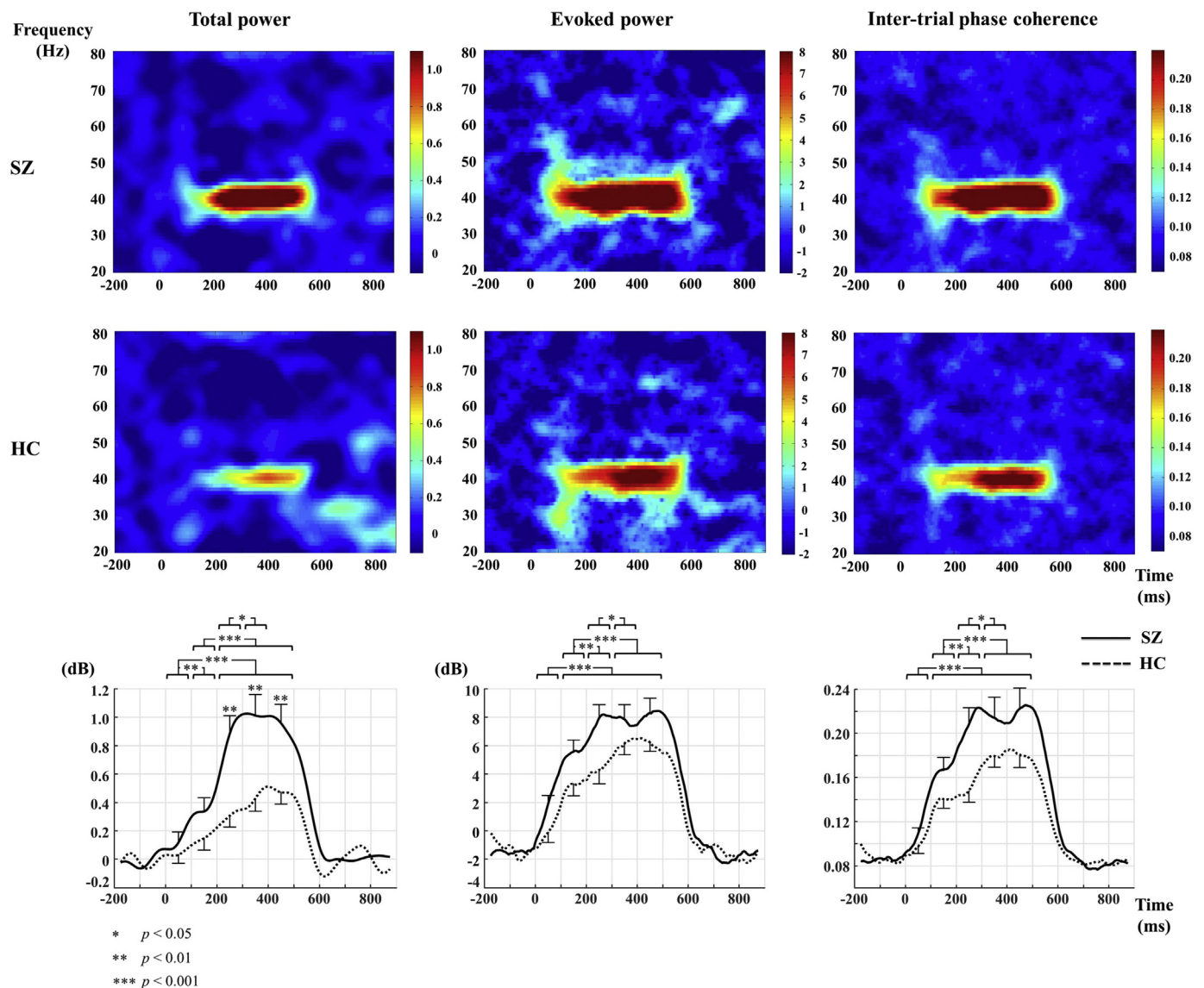
Fig. 1. The grand average of time-frequency maps and time course of total power, evoked power, and inter-trial phase coherence at Cz in the 40-Hz frequency for patients with SZ and HCs. Bars in the time course indicate the standard error. HC, healthy control; SZ, schizophrenia.

3.5. Regression analyses for ASSR measures at Cz and STG volume

Following the 5000 bootstrap resampling technique, there was only a finding for mean evoked power (0-500 ms) at Cz and the right STG, with simple effect analyses of a significant interaction term (R^2 = 0.224, F = 2.459, df = 51, p = 0.036) showing an association between evoked power at Cz and right STG volume in HCs but not in patients with SZ (see Fig. 2), a pattern observed after considering TIV, medication dose, and duration of illness. However, associations were not observed for total power or ITC at Cz. Furthermore, no associations were observed between STG source activity and STG volume.

3.6. Regression analyses for psychological measures and ASSR measures at Cz

Following the 5000 bootstrap resampling technique, there was only a finding for verbal fluency and mean evoked power (0-500 ms) at Cz, with simple effect analyses of a significant interaction term (R^2 = 0.223, F = 2.984, df = 52, p = 0.019) showing an association between verbal fluency and evoked power at Cz in patients with SZ but not in HCs (see Fig. 3), a pattern observed after considering medication

dose and duration of illness. However, associations were not observed for total power or ITC at Cz. Furthermore, no associations were observed between psychological measures and STG source activity.

4. Discussion

We examined group differences in the 40-Hz ASSR as well as associations between 40-Hz ASSR activity, brain structure, and cognitive ability in HC and patients with SZ. The SZ group showed a higher ITC and larger total power and evoked power than HCs at Cz. In addition, mean evoked power at Cz was significantly positively correlated with right STG volume in HCs but not in patients with SZ. The group differences in ASSR measures as well as the associations between ASSR measures and STG volume were only found in ASSR measures at Cz but not in STG source activity. Only a few studies have attempted ROI-based source localization of 40-Hz ASSR using EEG in SZ to date. One study showed no differences between patients with SZ and HCs on ASSR source activity but significant differences on ASSR sensor activity, results that are in line with the current results (Koenig et al., 2012). However, another study found significant differences between patients with SZ and HCs for ASSR source activity (Mulert et al., 2011). Few
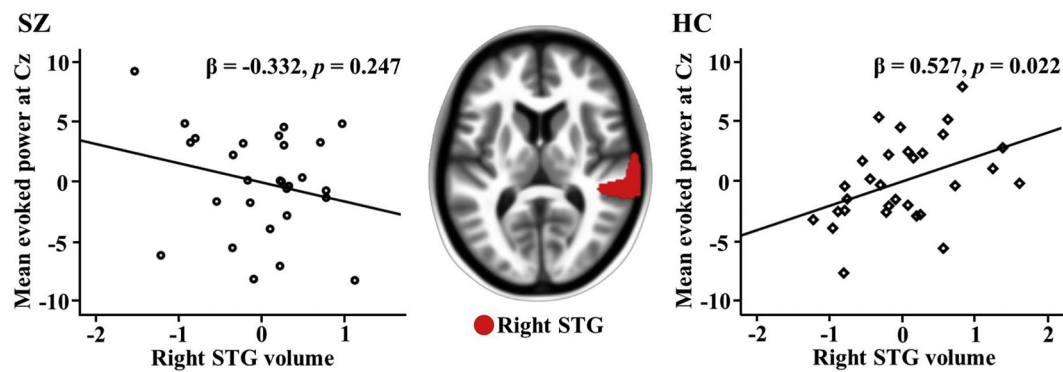
Fig. 2. The mean evoked power (0–500 ms) at Cz was significantly associated with right STG volume in HCs, while it was not significantly associated with right STG volume in patients with SZ. SZ: mean evoked power = − 1.602 * right STG volume – 0.002 * TIV – 0.002 * CPZ equivalent + 0.036 * duration of illness + 19.721 + error, HC: mean evoked power = 2.031 * right STG volume – 0.012 * TIV + 9.196 + error. CPZ, chlorpromazine; HC, healthy control; STG, superior temporal gyrus; SZ, schizophrenia; TIV, total intracranial volume.

studies that conducted source analysis of 40-Hz ASSR using MEG in SZ, found a group difference in STG source activity (Wilson et al., 2007) and a significant relationship between STG source activity and STG thickness (Edgar et al., 2014). Methodological aspects such as spatial resolution and the registration of individual MRI might have contributed to the differences in the results between the current study and the previous ones.

4.1. ASSRs

The current study found elevations in ITC and evoked power in SZ, whereas many of the previous studies have reported reductions in ITC and evoked power in SZ (Kwon et al., 1999; Roach et al., 2012; Wilson et al., 2008). While the reasons for this discrepancy are unclear, sample characteristics and different stimulus parameters might partly account for the current results. For example, while the present study included a relatively even percentage of male and female patients (female = 51.52%), many studies predominantly included male participants (Kwon et al., 1999; Spencer et al., 2009; Vierling-Claassen et al., 2008). Healthy female participants have been often found to exhibit higher oscillatory responses across several frequency ranges, including the gamma band (Güntekin and Başar, 2007; Jaušovec and Jaušovec, 2009). ASSR amplitudes and phase-locking measures may be influenced by female steroid hormones levels (Griskova-Bulanova et al., 2014; Zakaria et al., 2016) and interact with handedness (Melynyte et al., 2018). Although our post-hoc analysis did not reveal statistically significant sex differences in the 40-Hz ASSR measures in either SZ or HC, the effect of sex and its interaction with handedness needs to be investigated in the future. In addition, some studies have suggested an age effect on the 40-Hz ASSR measures (Edgar et al., 2018; Thuné et al., 2016). However, our study did not show a statistically significant correlation between age and 40-Hz ASSR measures in either group.
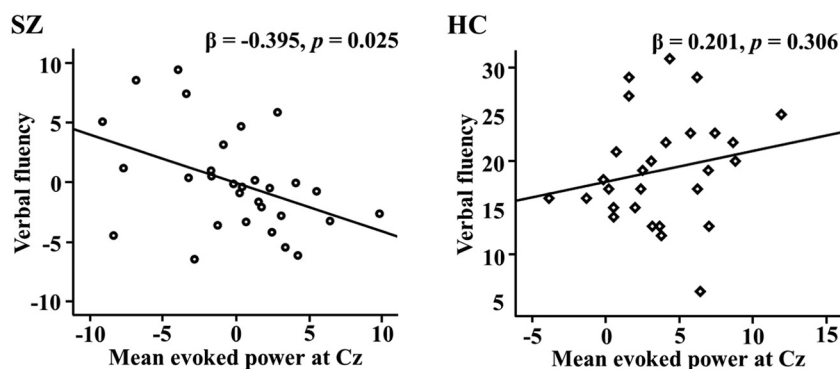
Moreover, we applied a longer inter-train interval (3050–3500 ms) than most previous studies (< 1000 ms). Interestingly, Hamm et al. (Hamm et al., 2012) employed a long ISI (~3000 ms) and reported higher ITC and larger induced and evoked power in the SZ than the HC group. The difference in ISI might explain our result of no group difference in baseline power as well. Several previous studies have reported increased baseline power during the 40-Hz ASSR in patients with SZ compared to HCs (Hirano et al., 2015; Spencer, 2012), but Hamm et al. (Hamm et al., 2012) and the current study did not confirm this finding. One possibility is that the relatively long ISI might make it more difficult to detect baseline power differences, since a longer ISI may better resemble the resting state as in the study of Hirano et al. (Hirano et al., 2015), which found no group differences in the resting-state power.

To investigate the effect of the length of inter-train interval on the results of the 40-Hz ASSR measures, we applied an ASSR paradigm with a 500-ms inter-train interval to eight patients with SZ and nine HCs for exploratory purposes (supplementary material). The exploratory analyses were conducted on Fz, FCz, and Cz electrodes. For the short inter-train interval, patients with SZ showed significantly reduced ITC compared to HCs. In addition, patients with SZ showed higher baseline power and lower total and evoked powers. It is possible that a long ISI will contribute to generation of the gamma band response by modulating the refractory time of pyramidal cells and interneurons in SZ.

Increased stimulus-induced gamma (i.e., total power) in this study corroborated the results of several previous studies (Hamm et al., 2012; Hirano et al., 2015; Teale et al., 2008). Teale et al. (Teale et al., 2008) found increased stimulus-induced gamma power in patients with SZ. Hirano et al. (Hirano et al., 2015) found that stimulus-induced gamma powers measured during the 40-Hz auditory steady state stimulation and task baseline were increased in patients with SZ compared with HCs. They suggested that enhanced gamma power in SZ may be a

Fig. 3. Mean evoked power (0–500 ms) was significantly correlated with verbal fluency in patients with SZ, while it was not significantly associated with verbal fluency in HCs. SZ: verbal fluency = − 0.407 * mean evoked power – 0.001 * CPZ equivalent – 0.165 * duration of illness + 21.204 + error, HC: verbal fluency = 0.333 * mean evoked power + 17.770 + error. CPZ, chlorpromazine; HC, healthy control; SZ, schizophrenia.

biomarker for the NMDAR dysfunction of fast-spiking inhibitory inter-neurons in neuropsychiatric disorders (Hirano et al., 2015). Interest-ingly, the group difference was not observed during the 0–100 ms period, indicating that the 40-Hz ASSR anomaly in SZ may not be ap-parent at the very early stage of the ASSR. This is consistent with the results of several other studies that found no difference in the 40-Hz ASSR in early latency (Edgar et al., 2014; Tada et al., 2014).

Increased gamma band ASSRs may be due to several factors in-cluding NMDAR dysfunction in SZ (Lazarewicz et al., 2010; Plourde et al., 1997; Sullivan et al., 2015), gray matter abnormalities (Edgar et al., 2014), GABA abnormalities (Vierling-Claassen et al., 2008), and the relatively old age of the participants in this study (Edgar et al., 2018). Furthermore, ketamine, in both humans and animals, increases evoked and total gamma power (Plourde et al., 1997; Vohs et al., 2012). In a recent study, the 40-Hz ASSR was both inhibited and disinhibited in the rodent brain depending on the temporal dynamics and the dose of NMDA antagonist used (Sivarao et al., 2016). This suggests the im-portance of carefully considering the experimental methods and parti-cipant characteristics that may modulate the 40-Hz ASSR measures in healthy and neuropsychiatric populations (Hudgens-Haney et al., 2017). Given the small magnitude of ASSR measure effect sizes reported in a recent meta-analysis (Thuné et al., 2016), the systematic in-vestigation of modulating factors may lead ASSR measures to become a definite biomarker of SZ.

A growing number of studies have reported that the 40-Hz ASSR is a complex phenomenon possibly modulated by factors such as sex and ISI, as mentioned above, as well as attentional demand (Griskova-Bulanova et al., 2018), antipsychotic medication status, and illness progression (Alegre et al., 2017; Tada et al., 2014). Therefore, future study would benefit from considering these multiple factors.

4.2. ASSRs and STG volume

Right STG volume was significantly positively correlated with mean evoked power at Cz only in HCs. This result is in line with a recent finding that the 40-Hz total power and ITC were positively correlated with left STG cortical thickness only in HCs (Edgar et al., 2014). Pa-tients with SZ may have lost this association due to brain anatomical alterations, such as reduced pyramidal cell volume in the STG deep layer (Sweet et al., 2003).

4.3. ASSRs and psychological measures

Patients with SZ had significantly lower scores in verbal fluency and verbal memory compared to HCs. Previous studies have shown that verbal fluency and verbal memory are the most impaired domains of cognitive function in SZ (Aleman et al., 1999; Cirillo and Seidman, 2003; Heinrichs and Zakzanis, 1998; Henry and Crawford, 2005). However, there was no group difference in the attentional task, in-dicating that the patients in this study might have had rather preserved attentional functions. In addition, high mean evoked power at Cz sig-nificantly correlated with poor verbal fluency in SZ. Few studies have reported an association between the 40-Hz ASSR and cognitive func-tion, including working memory (Light et al., 2006) and attention (Tada et al., 2014). Other studies, however, reported a null relationship (Kirihara et al., 2012). Our finding supports the idea that gamma os-cillatory deficits may be associated with cognitive dysfunction in SZ (Gonzalez-Burgos and Lewis, 2012).

4.4. Limitations

First, most patients with SZ had chronic illness and were receiving atypical antipsychotics. A previous longitudinal study found that cor-tical thinning was associated with higher cumulative antipsychotic in-take in patients with SZ (van Haren et al., 2011). Although we con-trolled the dosage of medication, future studies are warranted to assess

the duration of medication treatment and include drug-naive patients. Second, we examined the 40-Hz ASSR measures at Cz, which could be problematic as Cz measures combined left and right STG activity. Third, we included the entire STG as an ROI associated with the 40-Hz ASSR and did not constrain the analysis to the primary and secondary audi-tory cortices. Given the complexity of brain oscillations and the het-erogeneity of the pathophysiology of SZ, wider brain areas may be in-cluded as ROIs, where relevant.

5. Conclusion

Overall, this study demonstrated elevated gamma responses in SZ. The results were consistent with the NMDAR hypofunction model of SZ and supported other possibilities such as gray matter abnormalities and GABAergic dysfunction in SZ. Our finding suggested that the length of the ISI could be an important factor to consider with regard to the 40-Hz ASSR in SZ. Future studies, with sufficient statistical power, are needed to verify the observed tentative effect of the ISI length on the 40-Hz ASSR in patients with SZ and HCs. Furthermore, we found that right STG volume was related to the mean evoked power at Cz in the HC group, whereas patients with SZ did not show this association, possibly due to brain anatomical alterations. Finally, our results support the importance of gamma synchrony of the 40-Hz ASSR with cognition in SZ.

Author contributions

S.K. and S.K.J are co-first authors and equally contributed to this study. S.K. analyzed the data and wrote the paper. S.K.J collected the data and wrote the paper. D.W·K, M.S., and Y.W·K collected and ana-lyzed the data. S.H.L. designed the study and wrote the paper. S.H.L. and C.H.I. reviewed and revised the paper.

Conflict of interest

None.

Appendix A. Supplementary data

Supplementary data to this article can be found online at https://doi.org/10.1016/j.nicl.2019.101732.

References

Alegre, M., Molero, P., Valencia, M., Mayner, G., Ortuño, F., Artieda, J., 2017. Atypical antipsychotics normalize low-gamma evoked oscillations in patients with schizo-phrenia. Psychiatry Res. 247, 214–221.

Aleman, A., Hijman, R., de Haan, E.H., Kahn, R.S., 1999. Memory impairment in schi-zophrenia: a meta-analysis. Am. J. Psychiatr. 156, 1358–1366.

Ashburner, J., 2007. A fast diffeomorphic image registration algorithm. Neuroimage 38, 95–113.

Ashburner, J., 2009. Computational anatomy with the SPM software. Magn. Reson. Imaging 27, 1163–1174.

Ashburner, J., Friston, K.J., 2000. Voxel-based morphometry—the methods. Neuroimage 11, 805–821.

Ashburner, J., Friston, K.J., 2005. Unified segmentation. Neuroimage 26, 839–851.

Brett, M., Johnsrude, I.S., Owen, A.M., 2002. The problem of functional localization in the human brain. Nat. Rev. Neurosci. 3, 243.

Buzsáki, G., Wang, X.-J., 2012. Mechanisms of gamma oscillations. Annu. Rev. Neurosci. 35, 203–225.

Cirillo, M.A., Seidman, L.J., 2003. Verbal declarative memory dysfunction in schizo-phrenia: from clinical assessment to genetics and brain mechanisms. Neuropsychol. Rev. 13, 43–77.

Delorme, A., Makeig, S., 2004. EEGLAB: an open source toolbox for analysis of single-trial

EEG dynamics including independent component analysis. J. Neurosci. Methods 134, 9–21.

Dorph-Petersen, K.-A., Delevich, K.M., Marcsisin, M.J., Zhang, W., Sampson, A.R., Gundersen, H.J.G., Lewis, D.A., Sweet, R.A., 2009. Pyramidal neuron number in layer 3 of primary auditory cortex of subjects with schizophrenia. Brain Res. 1285, 42–57.

Edgar, J.C., Chen, Y.-H., Lanza, M., Howell, B., Chow, V.Y., Heiken, K., Liu, S., Wootton, C., Hunter, M.A., Huang, M., 2014. Cortical thickness as a contributor to abnormal oscillations in schizophrenia? NeuroImage: Clin. 4, 122–129.

Edgar, J., Fisk IV, C.L., Chen, Y.H., Stone-Howell, B., Liu, S., Hunter, M.A., Huang, M., Bustillo, J., Cañive, J.M., Miller, G.A., 2018. Identifying auditory cortex encoding abnormalities in schizophrenia: the utility of low-frequency versus 40 Hz steady-state measures. Psychophysiology 55 (8), e13074.

Ehrlichman, R., Gandal, M., Maxwell, C., Lazarewicz, M., Finkel, L., Contreras, D., Turetsky, B., Siegel, S., 2009. N-methyl-d-aspartic acid receptor antagonist–induced frequency oscillations in mice recreate pattern of electrophysiological deficits in schizophrenia. Neuroscience 158, 705–712.

First, M.B., Gibbon, M., Spitzer, R.L., Williams, J.B., 1996. User's Guide for the Structured Clinical Interview for DSM-IV Axis I Disorders—Research Version. Biometrics Research Department, New York State Psychiatric Institute, New York.

First, M.B., Gibbon, M., Spitzer, R.L., Benjamin, L.S., 1997. User's Guide for the Structured Clinical Interview for DSM-IV Axis II Personality Disorders: SCID-II. American Psychiatric Pub.

Fuchs, M., Kastner, J., Wagner, M., Hawes, S., Ebersole, J.S., 2002. A standardized boundary element method volume conductor model. Clin. Neurophysiol. 113, 702–712.

Goldman, H.H., Skodol, A.E., Lave, T.R., 1992. Revising axis V for DSM-IV: a review of measures of social functioning. Am. J. Psychiatry 149, 1148–1156.

Gonzalez-Burgos, G., Lewis, D.A., 2012. NMDA receptor hypofunction, parvalbumin-positive neurons and cortical gamma oscillations in schizophrenia. Schizophrenia Bull. 38 (5), 950–957.

Griskova-Bulanova, I., Griksiene, R., Korostenskaja, M., Ruksenas, O., 2014. 40 Hz auditory steady-state response in females: when is it better to entrain? Acta Neurobiol. Exp. 74, 91–97.

Griskova-Bulanova, I., Dapsys, K., Melynyte, S., Voicikas, A., Maciulis, V., Andruskevicius, S., Korostenskaja, M., 2018. 40 Hz auditory steady-state response in schizophrenia: sensitivity to stimulation type (clicks versus flutter amplitude-modulated tones). Neurosci. Lett. 662, 152–157.

Güntekin, B., Başar, E., 2007. Brain oscillations are highly influenced by gender differences. Int. J. Psychophysiol. 65, 294–299.

Gupta, C.N., Calhoun, V.D., Rachakonda, S., Chen, J., Patel, V., Liu, J., Segall, J., Franke, B., Zwiers, M.P., Arias-Vasquez, A., 2015. Patterns of gray matter abnormalities in schizophrenia based on an international mega-analysis. Schizophr. Bull. 41, 1133–1142.

Gutschalk, A., Mase, R., Roth, R., Ille, N., Rupp, A., Hähnel, S., Picton, T.W., Scherg, M., 1999. Deconvolution of 40 Hz steady-state fields reveals two overlapping source activities of the human auditory cortex. Clin. Neurophysiol. 110, 856–868.

Hamm, J.P., Gilmore, C.S., Clementz, B.A., 2012. Augmented gamma band auditory steady-state responses: support for NMDA hypofunction in schizophrenia. Schizophr. Res. 138, 1–7.

Haukoos, J.S., Lewis, R.J., 2005. Advanced statistics: bootstrapping confidence intervals for statistics with "difficult" distributions. Acad. Emerg. Med. 12, 360–365.

Heinrichs, R.W., Zakzanis, K.K., 1998. Neurocognitive deficit in schizophrenia: a quantitative review of the evidence. Neuropsychology 12, 426.

Henry, J., Crawford, J., 2005. A meta-analytic review of verbal fluency deficits in schizophrenia relative to other neurocognitive deficits. Cogn. Neuropsych. 10, 1–33.

Herdman, A.T., Lins, O., Van Roon, P., Stapells, D.R., Scherg, M., Picton, T.W., 2002. Intracerebral sources of human auditory steady-state responses. Brain Topogr. 15, 69–86.

Hirano, Y., Oribe, N., Kanba, S., Onitsuka, T., Nestor, P.G., Spencer, K.M., 2015. Spontaneous gamma activity in schizophrenia. JAMA Psychiatry 72, 813–821.

Hong, L.E., Summerfelt, A., McMahon, R., Adami, H., Francis, G., Elliott, A., Buchanan, R.W., Thaker, G.K., 2004. Evoked gamma band synchronization and the liability for schizophrenia. Schizophr. Res. 70, 293–302.

Hudgens-Haney, M.E., Ethridge, L.E., Knight, J.B., McDowell, J.E., Keedy, S.K., Pearlson, G.D., Tamminga, C.A., Keshavan, M.S., Sweeney, J.A., Clementz, B.A., 2017. Intrinsic neural activity differences among psychotic illnesses. Psychophysiology. 54 (8), 1223–1238.

Jadi, M.P., Behrens, M.M., Sejnowski, T.J., 2016. Abnormal gamma oscillations in N-methyl-D-aspartate receptor hypofunction models of schizophrenia. Biol. Psychiatry 79, 716–726.

Jaušovec, N., Jaušovec, K., 2009. Do women see things differently than men do? Neuroimage 45, 198–207.

Kantrowitz, J.T., Javitt, D.C., 2010. N-methyl-d-aspartate (NMDA) receptor dysfunction or dysregulation: the final common pathway on the road to schizophrenia? Brain Res. Bull. 83, 108–121.

Kay, S.R., Fiszbein, A., Opfer, L.A., 1987. The positive and negative syndrome scale (PANSS) for schizophrenia. Schizophr. Bull. 13, 261.

Kiebel, S.J., Tallon-Baudry, C., Friston, K.J., 2005. Parametric analysis of oscillatory activity as measured with EEG/MEG. Hum. Brain Mapp. 26, 170–177.

Kim, H., 1999. Rey-Kim Memory Test. Neuropsychology Press, Daegu, Korea.

Kim, Y.-R., Hwang, S.-T., Kim, S.-G., Lee, H.-S., 2015. Social function in patients with personality disorder diagnosed by single dimensional severity using Korean version of social functioning questionnaire. J. Kor. Neuropsych. Assoc. 54, 523–533.

Kim, J.S., Kim, S., Jung, W., Im, C.-H., Lee, S.-H., 2016. Auditory evoked potential could reflect emotional sensitivity and impulsivity. Sci. Rep. 6, 37683.

Kirihara, K., Rissling, A.J., Swerdlow, N.R., Braff, D.L., Light, G.A., 2012. Hierarchical

organization of gamma and theta oscillatory dynamics in schizophrenia. Biol. Psychiatry 71, 873–880.

Koenig, T., van Swam, C., Dierks, T., Hubl, D., 2012. Is gamma band EEG synchronization reduced during auditory driving in schizophrenia patients with auditory verbal hallucinations? Schizophr. Res. 141, 266–270.

Korotkova, T., Fuchs, E.C., Ponomarenko, A., von Engelhardt, J., Monyer, H., 2010. NMDA receptor ablation on parvalbumin-positive interneurons impairs hippocampal synchrony, spatial representations, and working memory. Neuron 68, 557–569.

Krishnan, G.P., Hetrick, W.P., Brenner, C., Shekhar, A., Steffen, A., O'Donnell, B.F., 2009. Steady state and induced auditory gamma deficits in schizophrenia. Neuroimage 47, 1711–1719.

Kwon, J.S., O'donnell, B.F., Wallenstein, G.V., Greene, R.W., Hirayasu, Y., Nestor, P.G., Hasselmo, M.E., Potts, G.F., Shenton, M.E., McCarley, R.W., 1999. Gamma frequency–range abnormalities to auditory stimulation in schizophrenia. Arch. Gen. Psychiatry 56, 1001–1005.

Lazarewicz, M.T., Ehrlichman, R.S., Maxwell, C.R., Gandal, M.J., Finkel, L.H., Siegel, S.J., 2010. Ketamine modulates theta and gamma oscillations. J. Cogn. Neurosci. 22, 1452–1464.

Lee, J.Y., Cho, M.J., Kwon, J.S., 2006. Global assessment of functioning scale and social and occupational functioning scale. Kor. J. Psychopharmacol. 17, 122–127.

Lewis, D.A., Curley, A.A., Glausier, J.R., Volk, D.W., 2012. Cortical parvalbumin interneurons and cognitive dysfunction in schizophrenia. Trends Neurosci. 35, 57–67.

Lezak, M.D., 2004. Neuropsychological Assessment. Oxford University Press, USA.

Light, G.A., Hsu, J.L., Hsieh, M.H., Meyer-Gomes, K., Sprock, J., Swerdlow, N.R., Braff, D.L., 2006. Gamma band oscillations reveal neural network cortical coherence dysfunction in schizophrenia patients. Biol. Psychiatry 60, 1231–1240.

Mathalon, D.H., Sohal, V.S., 2015. Neural oscillations and synchrony in brain dysfunction and neuropsychiatric disorders: it's about time. JAMA Psychiatry 72, 840–844.

McNally, J.M., McCarley, R.W., 2016. Gamma band oscillations: a key to understanding schizophrenia symptoms and neural circuit abnormalities. Curr. Opin. Psychiatry 29, 202–210.

Melynyte, S., Pipinis, E., Genyte, V., Voicikas, A., Rihs, T., Griskova-Bulanova, I., 2018. 40 Hz auditory steady-state response: the impact of handedness and gender. Brain Topogr. 1–11.

Moore, A., Gorodnitsky, I., Pineda, J., 2012. EEG mu component responses to viewing emotional faces. Behav. Brain Res. 226, 309–316.

Mulert, C., Kirsch, V., Pascual-Marqui, R., McCarley, R.W., Spencer, K.M., 2011. Long-range synchrony of gamma oscillations and auditory hallucination symptoms in schizophrenia. Int. J. Psychophysiol. 79, 55–63.

O'donnell, B.F., Hetrick, W.P., Vohs, J.L., Krishnan, G.P., Carroll, C.A., Shekhar, A., 2004. Neural synchronization deficits to auditory stimulation in bipolar disorder. Neuroreport 15, 1369–1372.

Pascual-Marqui, R.D., 2002. Standardized low-resolution brain electromagnetic tomography (sLORETA): technical details. Methods Find. Exp. Clin. Pharmacol. 24, 5–12.

Pernet, C.R., Chauveau, N., Gaspar, C., Rousselet, G.A., 2011. LIMO EEG: a toolbox for hierarchical LInear MOdeling of ElectroEncephaloGraphic data. Comput. Intell. Neurosci. 2011, 3.

Pernet, C.R., Wilcox, R.R., Rousselet, G.A., 2013. Robust correlation analyses: false positive and power validation using a new open source Matlab toolbox. Front. Psychol. 3, 606.

Picton, T.W., John, M.S., Dimitrijevic, A., Purcell, D., 2003. Human auditory steady-state responses: respuestas auditivas de estado estable en humanos. Int. J. Audiol. 42, 177–219.

Plourde, G., Baribeau, J., Bonhomme, V., 1997. Ketamine increases the amplitude of the 40-Hz auditory steady-state response in humans. Br. J. Anaesth. 78, 524–529.

Roach, B., Ford, J., Hoffman, R., Mathalon, D., 2012. Converging evidence for gamma synchrony deficits in schizophrenia. Suppl. Clin. Neurophysiol. 62, 163–180.

Ruscio, J., 2008. Constructing confidence intervals for Spearman's rank correlation with ordinal data: a simulation study comparing analytic and bootstrap methods. J. Mod. Appl. Stat. Methods 7, 7.

Salinas, E., Sejnowski, T.J., 2001. Correlated neuronal activity and the flow of neural information. Nat. Rev. Neurosci. 2, 539–550.

Segall, J.M., Turner, J.A., van Erp, T.G., White, T., Bockholt, H.J., Gollub, R.L., Ho, B.C., Magnotta, V., Jung, R.E., McCarley, R.W., 2008. Voxel-based morphometric multisite collaborative study on schizophrenia. Schizophr. Bull. 35, 82–95.

Semlitsch, H.V., Anderer, P., Schuster, P., Presslich, O., 1986. A solution for reliable and valid reduction of ocular artifacts, applied to the P300 ERP. Psychophysiology 23, 695–703.

Seo, E.H., Lee, D.Y., Kim, K.W., Lee, J.H., Jhoo, J.H., Youn, J.C., Choo, I., Ha, J., Woo, J.I., 2006. A normative study of the trail making test in Korean elders. Int. J. Geriatric Psychiatry 21, 844–852.

Sivarao, D.V., Chen, P., Senapati, A., Yang, Y., Fernandes, A., Benitex, Y., Whiterock, V., Li, Y.-W., Ahlijanian, M.K., 2016. 40 Hz auditory steady-state response is a pharmacodynamic biomarker for cortical NMDA receptors. Neuropsychopharmacology 41, 2232–2240.

Spencer, K.M., 2012. Baseline gamma power during auditory steady-state stimulation in schizophrenia. Front. Hum. Neurosci. 5, 190.

Spencer, K.M., Niznikiewicz, M.A., Nestor, P.G., Shenton, M.E., McCarley, R.W., 2009. Left auditory cortex gamma synchronization and auditory hallucination symptoms in schizophrenia. BMC Neurosci. 10, 85.

Sullivan, E.M., Timi, P., Hong, L.E., O'Donnell, P., 2015. Effects of NMDA and GABA-A receptor antagonism on auditory steady-state synchronization in awake behaving rats. Int. J. Neuropsychopharmacol. 18.

Sweet, R.A., Pierri, J.N., Auh, S., Sampson, A.R., Lewis, D.A., 2003. Reduced pyramidal cell somal volume in auditory association cortex of subjects with schizophrenia. Neuropsychopharmacology 28, 599.

Tada, M., Nagai, T., Kirihara, K., Koike, S., Suga, M., Araki, T., Kobayashi, T., Kasai, K., 2014. Differential alterations of auditory gamma oscillatory responses between pre-onset high-risk individuals and first-episode schizophrenia. Cereb. Cortex bhu278.

Tallon-Baudry, C., Bertrand, O., 1999. Oscillatory gamma activity in humans and its role in object representation. Trends Cogn. Sci. 3, 151–162.

Tallon-Baudry, C., Bertrand, O., Delpuech, C., Pernier, J., 1996. Stimulus specificity of phase-locked and non-phase-locked 40 Hz visual responses in human. J. Neurosci. 16, 4240–4249.

Teale, P., Collins, D., Maharajh, K., Rojas, D.C., Kronberg, E., Reite, M., 2008. Cortical source estimates of gamma band amplitude and phase are different in schizophrenia. Neuroimage 42, 1481–1489.

Thuné, H., Recasens, M., Uhlhaas, P.J., 2016. The 40-Hz auditory steady-state response in patients with schizophrenia: a meta-analysis. JAMA Psychiatry 73, 1145–1153.

Uhlhaas, P.J., Singer, W., 2010. Abnormal neural oscillations and synchrony in schizophrenia. Nat. Rev. Neurosci. 11, 100–113.

van Haren, N.E., Schnack, H.G., Cahn, W., van den Heuvel, M.P., Lepage, C., Collins, L., Evans, A.C., Pol, H.E.H., Kahn, R.S., 2011. Changes in cortical thickness during the course of illness in schizophrenia. Arch. Gen. Psychiatry 68, 871–880.

Vierling-Claassen, D., Siekmeier, P., Stufflebeam, S., Kopell, N., 2008. Modeling GABA alterations in schizophrenia: a link between impaired inhibition and altered gamma and beta range auditory entrainment. J. Neurophysiol. 99, 2656–2671.

Vohs, J.L., Chambers, R.A., O'Donnell, B.F., Krishnan, G.P., Morzorati, S.L., 2012. Auditory steady state responses in a schizophrenia rat model probed by excitatory/inhibitory receptor manipulation. Int. J. Psychophysiol. 86, 136–142.

Wilson, T.W., Hernandez, O.O., Asherin, R.M., Teale, P.D., Reite, M.L., Rojas, D.C., 2007. Cortical gamma generators suggest abnormal auditory circuitry in early-onset psychosis. Cereb. Cortex 18, 371–378.

Wilson, T.W., Hernandez, O.O., Asherin, R.M., Teale, P.D., Reite, M.L., Rojas, D.C., 2008. Cortical gamma generators suggest abnormal auditory circuitry in early-onset psychosis. Cereb. Cortex 18, 371–378.

Zakaria, M.N., Jalaei, B., Wahab, N.A.A., 2016. Gender and modulation frequency effects on auditory steady state response (ASSR) thresholds. Eur. Arch. Otorhinolaryngol. 273, 349–354.

Zanello, A., Weber, R.B., Gex-Fabry, M., Maercker, A., Guimon, J., 2005. Validation of the QFS measuring the frequency and satisfaction in social behaviours in psychiatric adult population. L'Encephale 32, 45–59.